Eddy Current Loss Estimation of Edge Burr affected Magnetic Laminations Based on Equivalent Electrical Network-Part II Analytical modeling and Experimental Results

Hamed Hamzehbahmani[1], Philip Anderson[1], Jeremy Hall[1] and David Fox[2]
[1]Wolfson Centre for Magnetics, Cardiff University, Cardiff CF24 3AA, UK
[2]Cogent Power Ltd., Newport NP19 0RB, UK

***Abstract*— In Part I of this two-part paper, fundamental concepts of inter-laminar fault and its consequences on magnetic cores were presented. An equivalent configuration, which was proved by FEM modelling, was proposed for magnetic cores with inter-laminar fault. In this Part II paper, based on the equivalent configuration of the core and equivalent circuit of eddy current path, an analytical model is developed to estimate eddy current power loss of magnetic cores with inter-laminar faults in a wide range of magnetising frequency. Important factors such as skin effect, non-uniform flux density distribution, complex relative permeability and non-linear relation of *B (H)*, which are often neglected in the literature, are highlighted. Packs of two, three and four Epstein size laminations of conventional grain oriented (CGO) were shorted together artificially to measure the extra power loss caused by the inter-laminar fault and support the analytical modeling. It was found that in the magnetic cores affected by inter-laminar fault, skin effect is a determinant factor in the magnetic properties determinations, even at low frequencies.**

Keywords: eddy current power loss, edge burr, inter-laminar fault, skin effect, complex relative permeability, high frequencies, loss separation.

1. INTRODUCTION

ELECTRICAL machines are widely used in industry and power systems. These machines are not free of faults and there is always a major concern related to faults especially between the laminations of their cores. The interest of the detection of such fault has grown because it is important to have the knowledge of the health of the core laminations in the alternator of power plants and transformers to improve maintenance, to estimate the machine life span, and to schedule core replacement operations [1]. Various methods have been developed to detect inter-laminar faults in magnetic cores, which have been used in research and industrial works [2-6]. Conventional systems utilising wattmeters have been used to measure the increase in the overall power loss of the magnetic cores when a few laminations are short-circuited on either side by applying artificial burrs [7-9]. Various methods have also been developed to measure the localised power loss around the burred area to investigate the effect of edge burrs on the localised heat and power loss [9-10].

Power loss in magnetic cores is separated into three components: the hysteresis loss, the eddy current loss and the anomalous or excess loss. Eddy current power loss of magnetic cores, depends on the properties, arrangement and the most important thickness of the material [11]. Eddy current power loss decreases by decreasing the laminations thickness, because it causes smaller eddy current loops in the laminations. On the other hand, hysteresis loss increases as lamination thickness decreases below 0.2 mm [12], which is related to pinning effects on the rough surface of the lamination becoming significant below 0.2 mm thickness. However since in this work laminations of 0.3 mm thickness are used, this content does not impact in the work. Since the inter-laminar faults change the configuration of the magnetic laminations, as shown in Figs 1-b and 1-c of Part I paper, the main effect of edge burrs in the magnetic cores is related to the eddy current distribution and hence the eddy current power loss in the burred laminations; which cannot be evaluated by the conventional methods. In addition, since the main cause of the eddy current is time-varying magnetic fields, it is necessary to take the skin effect phenomenon into account in related studies. In the study of magnetic properties, the eddy currents and the eddy current power loss of single strip laminations and magnetic cores without edge burr under high frequency magnetization, skin effect has been studied by many authors [13-17]. However in thin sheet magnetic laminations under low frequency magnetisation, e.g. power frequencies 50 Hz or 60 Hz, this effect is negligible due to the skin depth being significantly greater than the lamination thickness. But, in the presence of edge burrs on either side of the magnetic cores, the effective thickness of the burred laminations will increase and, even at low frequencies, the effective thickness might become greater than the skin depth and hence the skin effect becomes significant; which is not addressed in the previous works.

In this paper, an analytical model is proposed to estimate eddy current power loss of magnetic cores with inter-laminar fault based on the equivalent configuration of a magnetic core with inter-laminar fault and equivalent circuit of eddy current of the laminations. In this modeling, skin effect, non-uniform flux density distribution, complex relative permeability and non-linear relation of *B (H)* are highlighted. A technique is also developed to separate core loss components obtained from the experimental measurements of power losses over a wide frequency range to separate the eddy current power loss and compare to the analytical results.

2. EQUIVALENT CIRCUIT OF MAGNETIC LAMINATION

In the previous works, some analytical methods have been reported to predict the magnetic properties of magnetic cores based on equivalent circuits of the magnetic laminations [18-20]. Eddy current and hence eddy current power loss in the magnetic laminations can also be studied by modeling the eddy current path by an electric circuit in which the components depend on the steel properties and physical dimensions of the eddy current path. Fig 1-a shows a 3-D view of a magnetic lamination at a time-varying flux density ***B*** and Fig 1-b shows the equivalent electric circuit of the eddy current path.

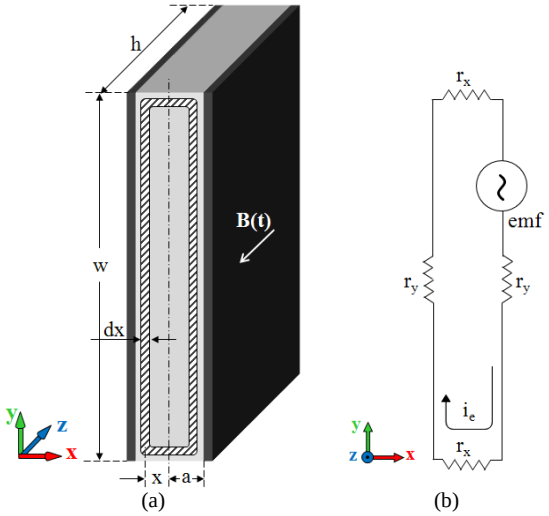

Fig 1 (a) Single strip lamination (b) equivalent electric circuit

In this figure, r_y and r_x are Ohmic resistances of the material along the width and thickness of the lamination respectively, which depend on the steel properties and physical dimensions of the eddy current path. The *emf* is an AC voltage source which represents the induced voltage in the lamination. Considering the partial area which is specified in Fig 1-a, the resistances of the eddy current path in the *x* and *y* directions are:

$$r_x = \rho \frac{l}{S} = \rho \frac{2a}{hdy} \tag{1}$$

$$r_y = \rho \frac{l}{S} = \rho \frac{w}{hdx} \tag{2}$$

Neglecting the resistance along the thickness r_x, the total resistance of the eddy current path is:

$$R_t = 2r_y = \rho \frac{2w}{hdx} \tag{3}$$

Therefore in a single magnetised lamination, power loss caused by the eddy current is equal to the power dissipated in the total resistance of R_t; and in a stack of magnetic laminations, with equal flux density in all of the laminations, the total eddy current power loss can be obtained by summing the power dissipated in each loop of the core laminations. However since the electrical steels are coated with insulating material on both sides, in order to develop a general equivalent circuit of magnetic cores it is necessary to take the effect of the inter-laminar insulating material into account.

The surface coating of the electrical steels are made of high resistance materials to limit the inter-laminar eddy current in the cores, from this point of view the effect of the inter-laminar coating can be considered as a large resistance [20]. On the other hand, it is well known that a capacitance consists of two conducting sheets which are insulated by a di-electric plate. From this point of view, in a stack of magnetic laminations adjacent laminations form a capacitance [18]. Therefore in order to develop an equivalent network for magnetic cores, the effect of inter-laminar insulating material could be considered in two different ways: considering the inter-laminar resistance between two adjacent laminations which lead to a pure resistive equivalent network or considering the inter-laminar capacitance between two adjacent laminations which lead to an *RC* equivalent network. Fig 2-a shows a stack of magnetic laminations under time-varying flux density ***B*** in rolling direction and Figs 2-b and 2-c show the pure resistive and *RC* equivalent networks of the core, respectively. R_2 and C_2 represent the equivalent inter-laminar resistance and capacitance between two adjacent laminations, respectively. Different techniques are available to measure these parameters [21-24].

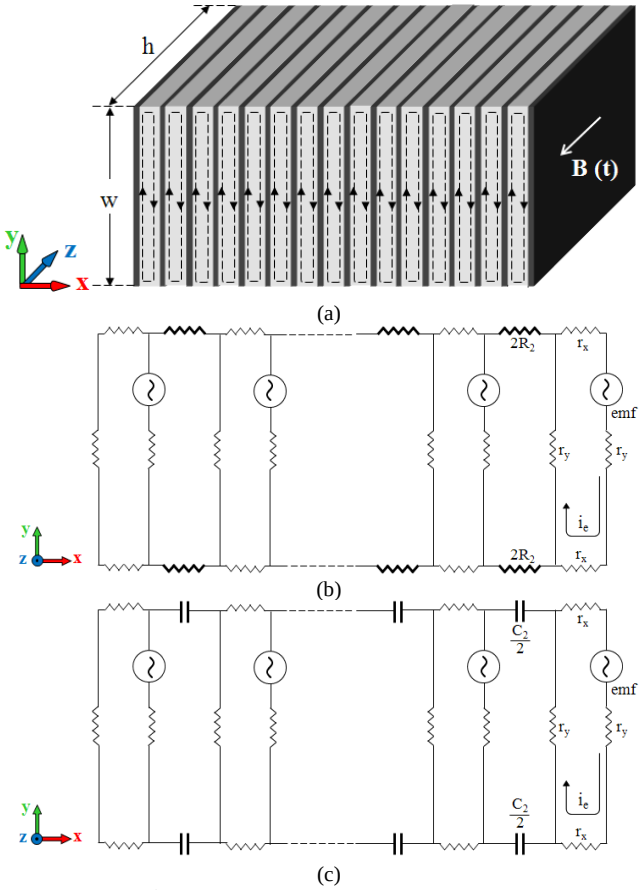

Fig 2 (a) Stack of magnetic lamination (b) pure resistive equivalent electric network (c) RC equivalent electric network

2.1. Induced emf in magnetised laminations

The total induced *emf* along the path indicated in Fig 1-a can be obtained by Faraday's law:

$$e_{ind} = -\frac{d\varphi}{dt} = -\frac{d(BA)}{dt} \tag{4}$$

The area of the path indicated in the Fig 1-a is $A=2xw$, therefore equation (4) can be written as:

$$e_{ind} = -\frac{d(B_z(x,t) \times A)}{dt} = -(2xw)\frac{d(B_z(x,t))}{dt} \qquad (5)$$

Substituting $B_z(x,t)$ from equation (3) of the Part I paper into (5) will result in:

$$e_{ind} = (2xwB_s\omega)\sqrt{\frac{\left(cosh\ \frac{2x}{\delta} + cos\ \frac{2x}{\delta}\right)}{\left(cosh\ \frac{2a}{\delta} + cos\ \frac{2a}{\delta}\right)}}\ Sin(\omega t - \beta) \qquad (6)$$

And the *rms* induced voltage in the lamination is obtained as:

$$e_{rms} = \sqrt{2}\pi f 2xwB_s\sqrt{\frac{\left(cosh\ \frac{2x}{\delta} + cos\ \frac{2x}{\delta}\right)}{\left(cosh\ \frac{2a}{\delta} + cos\ \frac{2a}{\delta}\right)}} \qquad [V] \qquad (7)$$

Equation (7) is a general equation for the induced voltage in the magnetised lamination which is a function of x, f and δ. However at low frequencies where $a/\delta<1$ and skin effect is negligible, the quantity under the square root of this equation approaches unity and the induced voltage in the lamination can be reduced to:

$$e_{rms} = \sqrt{2}\pi f 2xwB_s \qquad [V] \qquad (8)$$

Equation (8) can also be obtained by substituting equation (4) of the Part I paper into (5). Equations (7) and (8) show the *rms* induced *emf* in the magnetised lamination as a function of the distance from the centre line of the lamination. Equation (8), which is valid only at low frequencies, shows that the induced *emf* in the lamination is a linear function of x; due to the uniform distribution of the flux density along the lamination thickness and negligible skin effect at low frequencies. However the induced voltage in the laminations at high frequencies, equation (7), is not a linear function of x; because at high frequencies flux density distributes non-uniformly and also skin effect is noticeable.

3. EDDY CURRENT POWER LOSS MODELING BASED ON THE EQUIVALENT CIRCUIT OF THE MAGNETIC LAMINATION

By defining the resistance of the eddy current path and the induced voltage in the magnetised lamination properly, the induced eddy current and consequently the eddy current power loss could be calculated based on the governing equations of the electric circuit theory. However, in order to extend the modeling to a wide range of magnetising frequency and flux density, the effect of these two quantities on the model were considered; the details are discussed here.

3.1. Eddy current power loss modeling

Based on the equivalent circuit of the Fig 1-b, the eddy current in the specified path of the Fig 1-a can be obtained as:

$$di_e = \frac{e_{rms}}{R_t} \qquad (9)$$

Substituting the induced voltage from (7) into (9) leads to:

$$di_e = \frac{\sqrt{2}\pi f x B_s h}{\rho}\sqrt{\frac{\left(cosh\ \frac{2x}{\delta} + cos\ \frac{2x}{\delta}\right)}{\left(cosh\ \frac{2a}{\delta} + cos\ \frac{2a}{\delta}\right)}}\ dx \qquad (10)$$

Therefore the eddy current power loss of the specified path of the Fig 1-a is:

$$dp_e = \frac{4\pi^2 f^2 B_s^2 wh}{\rho}\left(\frac{cosh\ \frac{2x}{\delta} + cos\ \frac{2x}{\delta}}{cosh\ \frac{2a}{\delta} + cos\ \frac{2a}{\delta}}\right)x^2 dx \qquad (11)$$

And hence, the total eddy current power dissipated in the whole of the lamination can be obtained by integrating (11) from *0* to *+a*:

$$p_e = \frac{\pi^2 f^2 B_s^2 wh\delta^3}{2\rho\left(cosh\ \frac{2a}{\delta} + cos\ \frac{2a}{\delta}\right)}\left[\frac{4a}{\delta}\left(cos\ \frac{2a}{\delta} - cosh\ \frac{2a}{\delta}\right) + sinh\frac{2a}{\delta}\left(\left(\frac{2a}{\delta}\right)^2 + 2\right) + sin\frac{2a}{\delta}\left(\left(\frac{2a}{\delta}\right)^2 - 2\right)\right] \qquad (12)$$

Equation (12) is a general equation which describes the total eddy current power loss of thin sheet laminations of length h, width w and thickness $2a$ (in Watts) based on the resistive equivalent circuit of the magnetic lamination. In this equation the effect of non-uniform flux density distribution along the thickness of the lamination and also skin effect have been considered at high magnetising frequencies. However at low frequencies where $a/\delta<1$ and skin effect is negligible, the equation of (12) tends to:

$$p_e = \frac{4\pi^2 f^2 B_m^2 wha^3}{3\rho} \qquad [W] \qquad (13)$$

Equation (13) has been known as the conventional equation of eddy current power loss of thin sheet laminations at low frequencies. This equation can be also obtained by substituting the induced voltage from (8) for low frequencies into (9), in the calculation of the eddy current power loss.

In section 4 of the Part I paper, it was proved that in magnetic cores with inter-laminar fault skin effect becomes significant and flux density distributes non-uniformly along the equivalent thickness of the core. Therefore in calculation of eddy current power loss of magnetic cores with inter-laminar fault, equation (12) should be used, even at low frequencies; because in this equation, skin effect and non-uniform flux density distribution have been taken into account. Using equation (13) to calculate eddy current power loss of magnetic cores with an inter-laminar fault will be an overestimate; because this equation is based on a uniform flux density distribution and negligible skin effect.

4. EDDY CURRENT POWER LOSS SEPARATION

In order to validate the analytical modeling, an accurate and reliable experimental method is needed to separate the eddy current power loss from the total core power loss. An experimental-analytical method was developed to separate the components of core loss in a wide range of frequencies; the details are presented in this section.

4.1. Extrapolation method

Since the 19th century, iron core losses due to alternating fields have been separated into two main categories: hysteresis losses p_h and eddy current losses p_e [25]. However definition of core loss by these two terms gives large discrepancies compared to the experimental results, especially at high frequencies and high frequencies. This difference is normally explained by excess or anomalous loss. Bertotti [26] proposed an additional term to explain these excess losses based on the statistical loss theory, and the total core loss is expressed as:

$$p_c = p_h + p_e + p_a$$
$$= k_h f B_{pk}^n + k_e (f B_{pk})^2 + k_{ex} (f B_{pk})^{1.5} \quad (14)$$

where f is magnetising frequency, B_{pk} is peak flux density, n is a constant, k_h, k_e and k_{ex} are hysteresis, eddy current and excess loss coefficients, respectively. Calculating the coefficients of (14) leads to separation of the components of the iron loss. An analytical method, which is known as the *extrapolation method*, is usually used to separate the components of core loss using total core loss measurements at different frequencies. In this method, the hysteresis loss is separated by extrapolating core loss per cycle versus frequency curves at different flux densities to zero frequency [27]. Therefore dividing (14) by frequency f leads to:

$$\frac{p_c}{f} = \frac{p_h}{f} + \frac{p_e}{f} + \frac{p_a}{f}$$
$$= k_h B_{pk}^n + k_e f B_{pk}^2 + k_{ex} \sqrt{f} B_{pk}^{1.5} \quad (15)$$

And in term of constant coefficients:

$$\frac{p_c}{f} = D + Ef + G\sqrt{f} \quad (16)$$

Where $D = k_h B_{pk}^n$, $E = k_e B_{pk}^2$ and $G = k_{ex} B_{pk}^{1.5}$ are hysteresis power loss per cycle, eddy current power loss per cycle and excess power loss per cycle, respectively. Equation (16) can be plotted versus frequency f and a powerful solver is available within Microsoft Excel to solve the equation and determine the coefficients of D, E and G. However in [27-28] an alternative method is used to obtain the coefficients of (16) in which the total core loss data are used to plot curves of P_c/f versus square root of frequency $\sqrt{f}$, not frequency f, for different values of flux density from the lowest frequency to the highest frequency. Therefore (16) can be represented by:

$$\frac{p_c}{f} = D + E(\sqrt{f})^2 + G\sqrt{f} \quad (17)$$

where the coefficients of core loss components D, G and E can be obtained by polynomial curve fitting.

As a practical example, experimental results of total power loss of an Epstein size single strip lamination of CGO was measured at peak flux density 1.7 T and magnetising frequency from 10 Hz to 1000 Hz. Total power loss per cycle versus square root of frequency of this sample is shown in Fig 3. The polynomial function of this curve was obtained by using the polynomial solver of Microsoft Excel, as shown in the figure.

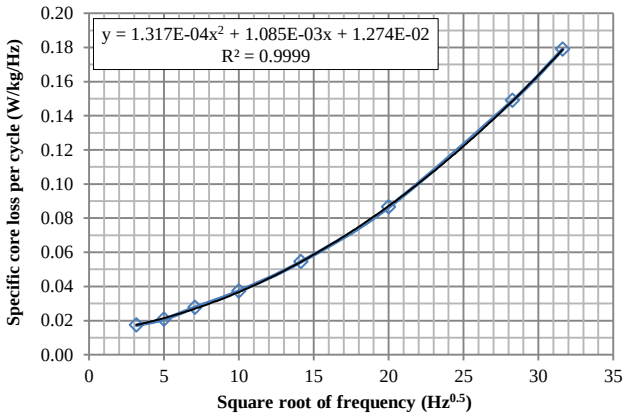

Fig 3 Total power loss of an Epstein size magnetic lamination per cycle versus square root of frequency at 1.7 T

The value of the fitting residual of the equation is very close to unity, i.e. R^2=0.9999, which indicates a very good approximation. Based on the coefficients of Fig 3, the components of the core loss at different frequencies were calculated and the results are shown in Table I.

Table I Core loss components of an Epstein size lamination of CGO at 1.7 T and different magnetising frequencies

f (Hz)	Measured loss (W/kg)	P_e (W/kg)	P_h (W/kg)	P_a (W/kg)
10	0.173	0.013	0.127	0.034
25	0.520	0.083	0.318	0.136
50	1.38	0.330	0.635	0.384
100	3.73	1.32	1.27	1.08
200	10.9	5.28	2.54	3.07
400	34.6	21.1	5.08	8.68
800	119	84.5	10.2	24.6
1000	178	132	12.7	34.3

As outlined initially, the extrapolation method is based on a constant hysteresis power loss per cycle and a linear relation of the eddy current power loss per cycle for all frequencies. However, from equation (3) and Fig 7 of the Part I paper it can be concluded that the local hysteresis loop and hence the hysteresis power loss per cycle at high frequencies varies at each point inside the lamination. This variation affects the total hysteresis power loss per cycle, making it dependent on the magnetic field distribution, which is strongly affected by the skin effect, magnetising frequency and peak flux density. Therefore the assumptions of the extrapolation method are only valid at low frequencies ($a/\delta<1$) and the coefficients of core loss components are not constant when the frequency changes.

4.2. Developed extrapolation method

To improve the coefficient of eddy current loss at high frequencies, a dimensionless correction coefficient (CC) was defined at each frequency and each flux density as:

$$CC = \frac{B_{av}}{B_s} \quad (18)$$

where B_s is the flux density at the surface of the lamination and B_{av} is the average value of flux density inside the lamination which is defined by:

$$B_{av} = \frac{1}{2a}\int_{-a}^{a} B_z(x)\,dx \qquad (19)$$

where $2a$ is thickness of the lamination and $B_z(x)$ is flux density as a function of distance from the centre line of the lamination which was defined by equation (3) in the Part I paper. Eddy current power loss obtained from the extrapolation method will be then multiplied by the CC defined by equation (18). As a practical example on implementing this method, the total power loss of a single strip Epstein size magnetic lamination with 0.3 mm thick of CGO 3% *SiFe* at flux densities 1.3 T, 1.5 T and 1.7 T and magnetising frequencies from 10 Hz to 1000 Hz was measured by using a single strip tester; the results are shown in Table II.

Table II Total power loss of an Epstein size lamination of CGO

Magnetising frequency (Hz)	Total power loss (W/kg)		
	1.3 T	1.5 T	1.7 T
10	0.074	0.107	0.173
25	0.244	0.342	0.520
50	0.674	0.946	1.38
100	1.92	2.61	3.73
200	5.67	7.72	10.9
400	17.5	24.4	34.6
800	57.7	82.8	119
1000	85.6	124	178

Based on equations (18) and (19) the correction coefficients of the eddy current power losses of this sample were calculated at each flux density, the results are shown in Fig 4.

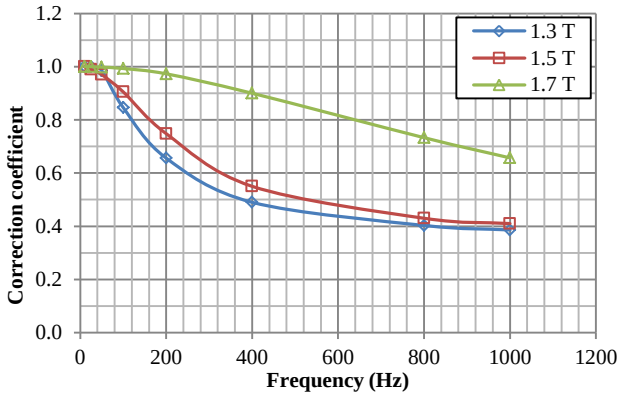

Fig 4 Correction coefficient of eddy current power loss of single strip Epstein size lamination of CGO

The results represented in Fig 4 show that the correction coefficient is close to unity at low frequencies and it decreases by increasing the frequency, which is related to effect of high frequencies on flux density. Eddy current power loss per cycle of this specimen was calculated by both the extrapolation and the developed extrapolation methods and the results were compared with that of equation (12). The results together with the difference between them typically at flux density 1.7 T are shown in Fig 5. The correction coefficient curves of Fig 4 were used in the loss separation and the complex relative permeability and the non-linear relation of *B (H)* were considered to predict the power losses.

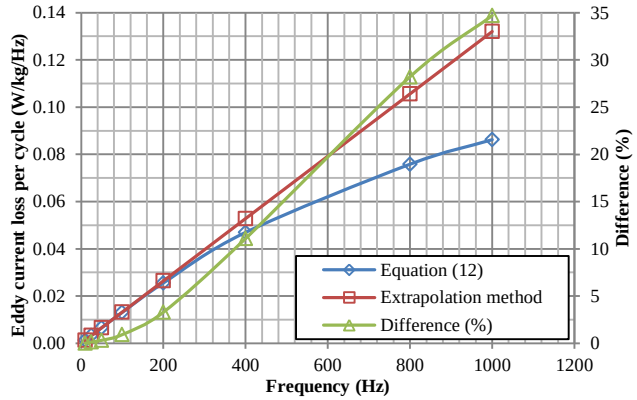

(a)

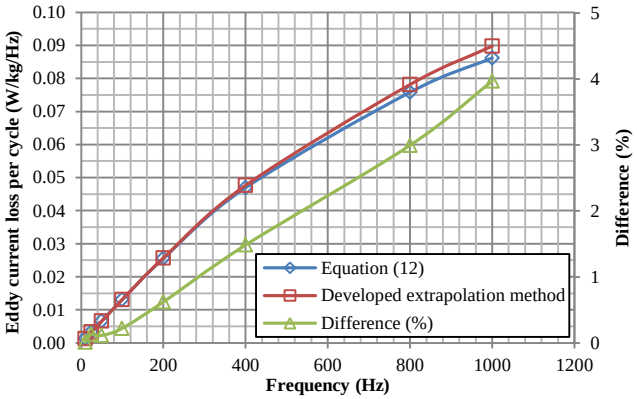

(b)

Fig 5 Eddy current power loss per cycle of an Epstein size lamination at 1.7 T from the equation (12) and (a) extrapolation method (b) developed extrapolation method

From the results represented in Fig 5-a, there is a close agreement between the eddy current power losses per cycle from equations (12) and the extrapolation method at low frequencies; however the difference between these two values increases by increasing the frequency, where at 1000 Hz the difference is about 35 %. On the other hand, Fig 5-b shows a close agreement between the results of the analytical modeling of equation (12) and the developed extrapolation method at all frequencies, with the maximum difference less than 4 % at magnetising frequency of 1000 Hz. Therefore the developed extrapolation method is a reliable method to separate power loss components in a wide range of magnetising frequency.

5. EDDY CURRENT POWER LOSS IN STACK OF BURRED LAMINATIONS BASED ON THE EQUIVALENT NETWORK

Based on the equivalent circuit of single strip lamination and the impedance of the inter-laminar material between two adjacent laminations, two possible equivalent networks, pure resistive and *RC* network, were developed for magnetic cores in section 2. However, since the insulation coating used in electrical steels is quite thin, the resulting capacitance between two adjacent laminations has a large value; e.g. for Epstein size strip (300mm×30mm) with approximately 3 µm insulation on both sides, the equivalent capacitance between two adjacent laminations is in the range of 5 nF [21]; and hence the equivalent capacitive reactance X_c, typically at power frequency of 50 Hz is about 0.637 MΩ. The magnetic field due

to inter-laminar capacitive currents was solved in [30] and the result shows that the inter-laminar capacitive currents are negligible below 20 MHz for laminated cores in electrical machines. On the other hand, coating material of the electrical steels has a large resistivity to limit the inter-laminar eddy current and hence the inter-laminar resistance of the electrical steels has a large value; e.g. for electrical steel coated with inorganic insulating coatings having surface insulation resistivities in excess of 30 KΩ-mm^2 [22]. Therefore compared to the resistance of the steel, which is in the range of μΩ, impedance (resistive or capacitive) of the inter-laminar coating is extremely large and it does not affect the eddy currents in the lamination loops. Therefore in a stack of laminations without burr, the total eddy current power loss at low frequencies could be calculated as $P_t=n\times P_1$; where n is number of the laminations and P_1 is the eddy current power loss of one single lamination. On the other hand, in the presence of edge burr on both sides of the magnetic cores the inter-laminar impedances are short-circuited by the edge burrs and all of the damaged laminations form one loop in the equivalent circuit of the core, as shown in section 4 of Part I paper.

5.1. Modeling of the inter-laminar short circuit

In this work, packs of two, three and four laminations of Epstein size 0.3 mm thick CGO 3% *SiFe* laminations were short circuited together artificially by melting lead-free solder in a soldering bath and putting the lamination sides into the bath. To prevent the solder penetrating between the laminations two iron strips of 5 mm thickness were used to clamp the laminations on either side. Fig 6 shows cross section view of the pack of four shorted laminations.

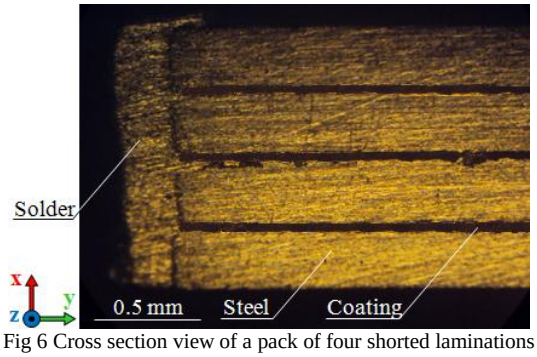

Fig 6 Cross section view of a pack of four shorted laminations

In section 3.2 of Part I paper using equation (7) general condition of effect of high frequencies on the complex relative permeability was taken into account up to 1 MHz. However in section 4.2 of that paper it was stated that in presence of edge burr on either sides of laminations effect of frequency changes on the complex relative permeability extremely reduces, e.g. this effect was reduced to a few hertz in the case of four shorted laminations, as shown in Fig 17. Therefore, in the experimental part of this work, the samples were magnetised up to 1 KHz; because within this frequency range effect of frequency on complex relative permeability is obvious.

The specific core loss of the packs of two, three and four burred laminations were measured at flux densities 1.3 T, 1.5 T and 1.7 T and magnetising frequency from 10 Hz up to 1 kHz. The results of the measurements that accompany the results of single strip laminations at flux densities 1.3 T, 1.5 T and 1.7 T and magnetising frequencies 10 Hz, 50 Hz, 100 Hz, 200 Hz, 400 Hz and 1000 Hz are shown in Fig 7. A significant increase in the power losses of the single strip lamination and shorted laminations can be observed from Fig 7; for example specific loss at 1.7 T and 1000 Hz for a single strip lamination and the pack of four shorted laminations increased from 178.9 W/Kg to approximately 2000 W/Kg.

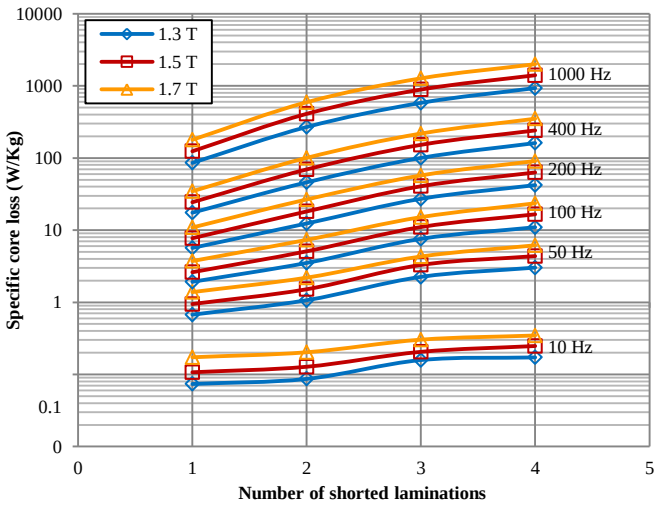

Fig 7 Specific core loss versus number of shorted laminations at different flux densities and frequencies

The power loss components were separated at each flux density and frequency based on the developed extrapolation method described in section 4. As an example, the results of the power loss measurement of two shorted laminations at 1.7 T are shown in Table III. Comparing the results shown in Table III with that of single strip lamination of Table I leads to an interesting conclusion.

Table III Core loss components of a pack of two burred lamination at 1.7 T and different magnetising frequencies

f (Hz)	Measured loss (W/kg)	P_e (W/kg)	P_h (W/kg)	P_a (W/kg)
10	0.203	0.056	0.114	0.023
25	0.729	0.349	0.285	0.091
50	2.19	1.40	0.569	0.258
100	7.32	5.59	1.14	0.729
200	26.6	22.4	2.28	2.06
400	100	89.4	4.55	5.83
800	384	357	9.11	16.5
1000	592	559	11.4	23.1

Compared to the single strip lamination the hysteresis loss of the two shorted laminations, which could be considered as a single lamination of 0.6 mm thickness, is decreased slightly, but the eddy current loss is increased significantly; because these two components of core loss have different natures. For a given material and flux density the hysteresis loss depends only on the mass of the material, while the eddy current loss depends on the sheet thickness, electrical resistivity and arrangement of the material. Thus in a burred core, due to the

very thin thickness of the coating between the shorted laminations, the hysteresis loss decreases slightly. On the other hand based on the hypothesis described in section 4 of Part I paper, the inter-laminar short leads to bigger eddy current loop in the shorted laminations and change the configuration of the shorted laminations as a solid core which in turn leads to higher eddy current loss.

5.2. Analytical modeling of the inter-laminar short circuit

Eddy current power losses of the shorted laminations based on equation (12) and taking into account the non-linear relation of *B (H)* and also complex relative permeability of the material were predicted. Correction coefficients of eddy current power loss were calculated from equations (18) and (19) at each frequency and each flux density. Typical result of the CC for the pack of two shorted laminations is shown in Fig 8.

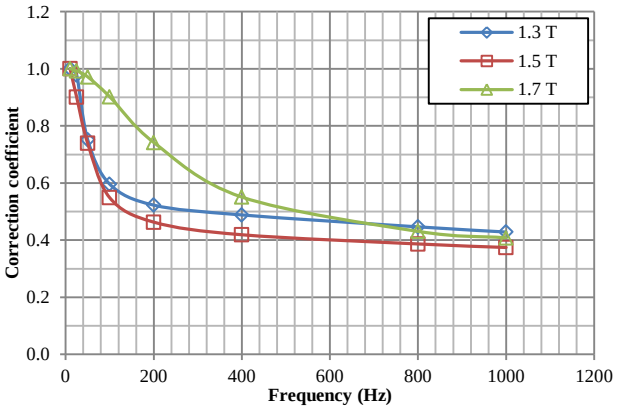

Fig 8 Correction coefficient of eddy current power loss of pack of two shorted laminations

The eddy current power loss was separated at each flux density and frequency based on the extrapolation method developed here and the results were compared with the prediction results from the analytical modeling. The final results including the packs of two, three and four shorted laminations together with the result of single strip lamination at flux densities 1.3 T, 1.5 T and 1.7 T and magnetising frequency from 10 Hz to 1000 Hz are shown in Figs 9. Compared to the eddy current power loss of the single strip lamination in normal condition, Fig 9-a, eddy current power loss caused by the inter-laminar fault is extremely high which demonstrates the importance of edge burr removal on the core losses and hence the transformer efficiency.

In the case of single strip lamination, a close agreement with the maximum difference of less than 4 % was found between the prediction and experimental results. On the other hand in the case of shorted laminations the maximum difference between the prediction and experimental results at magnetising frequencies up to 400 Hz was about 6 %; however at higher frequencies the difference was increased to about 10 %. Regarding the experimental conditions and the base of the analytical modeling, the difference could be related to the following issues:

- In the analytical model a solid core with thickness of *2na* was assumed; while in the practical measurements the laminations are separated by the inter-laminar coating.

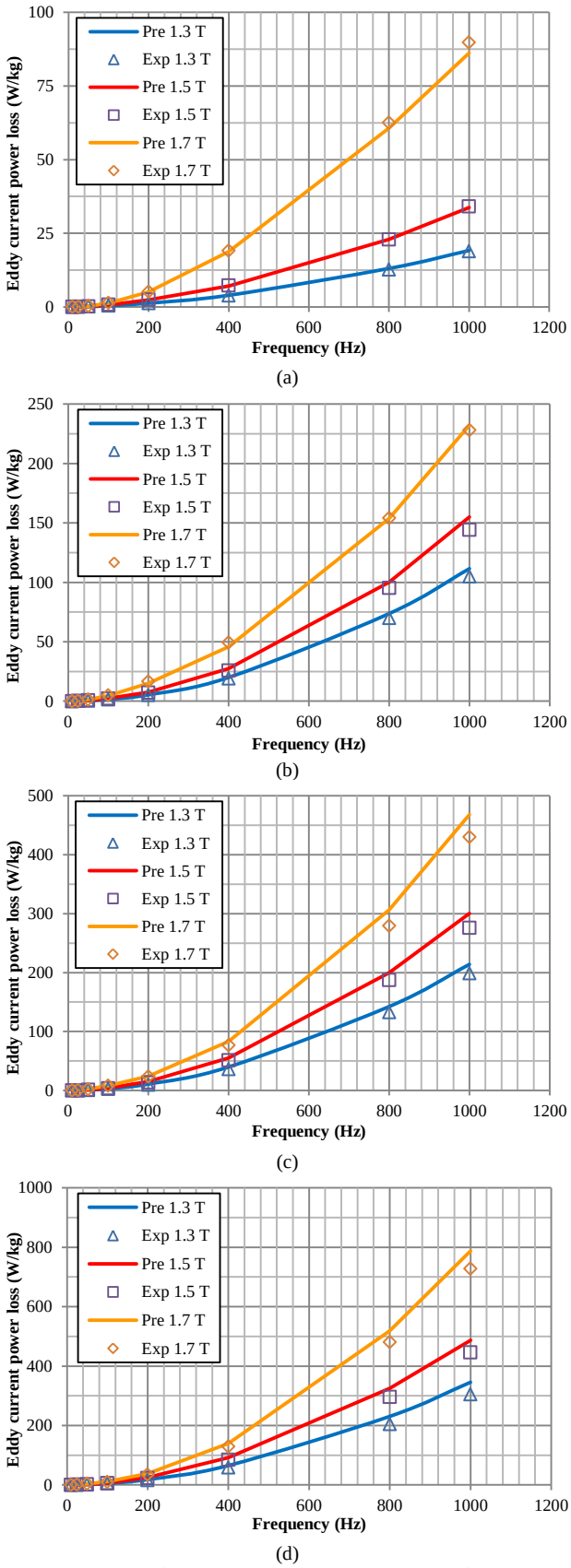

Fig 9 Comparison of prediction and experimental results of eddy current power loss of (a) single strip Epstein size lamination and packs of (b) two (c) three (d) four shorted laminations at flux densities 1.3 T, 1.5 T and 1.7 T

- In the analytical modeling a solid core with uniform electrical property was considered; however in the experimental work, the laminations were shorted by lead free solder with conductivity of 7.69×10^6 S/m which is about 3.5 times greater than conductivity of the steel.

Since the analytical model is based on the physical dimensions of the laminations, it is possible to develop the model to decrease the discrepancy by taking into account the effect of the shorted edges and the inter-laminar coating.

6. CONCLUSION

In this paper an equivalent circuit model was proposed for the magnetised laminations to calculate and predict the eddy current power loss. In this model, skin effect, non-uniform flux density distribution, complex relative permeability and the non-linear *B (H)* characteristic have been considered; therefore the proposed model provides accurate loss calculation for a wide range of flux density and magnetising frequency. This model is applicable for laminated magnetic cores with or without burr. Based on analytical modeling, it was found that the skin effect is a key factor in the eddy current power loss investigation in magnetic cores not only at high frequencies, but also at low frequencies when the core is affected by the edge burr. In order to support the analytical modeling, packs of two, three and four Epstein size CGO laminations were shorted together artificially and the total power loss was measured by using a single strip tester. An experimental-analytical method was also developed to separate eddy current power loss from the measured total loss in a wide range of frequencies.

ACKNOWLEDGMENT

The authors are grateful to Cogent Power Ltd. for providing the electrical steel sheets.

REFERENCES

[1] R Romary, C Demian, P Schlupp, J Y Roger, T Szkudlapski "Real Scale Experimental Devices for Stator Core Fault Analysis", International Symposium on Diagnostics for Electric Machines, Power Electronics & Drives, 2011, pp 71-76

[2] C A Schulz, S Duchesne, D Roger and J N Vincent "Short Circuit Current Measurements between Transformer Sheets", IEEE Trans Magn, VOL. 46, NO. 2, Feb 2010, pp 536-539

[3] S B Lee, G Kliman, M Shah, D Kim, T Mall, K Nair and M Lusted, "Experimental Study of Inter-laminar Core Fault Detection Techniques based on Low Flux Core Excitation" IEEE Trans On Energy Convers, VOL. 21, NO. 1, March 2006, pp 85-94

[4] S B Lee, G B Kliman, M R Shah, N K Nair and R M Lusted "An iron core probe based inter-laminar core fault detection technique for generator stator cores" IEEE Trans Ener Conv, Vol 20, No 2, Jun 2005, pp. 344–351

[5] S B Lee, G B Kliman, M R Shah, W T Mall, N K Nair and R M Lusted "An advanced technique for detecting inter-laminar stator core faults in large electric machines" IEEE Trans On Ind. App, VOL. 41, NO. 5, Sep/Oct 2005, pp. 1185–1193

[6] G B Kliman, S. B. Lee, M. R. Shah, R. M. Lusted, and N. K. Nair, "A new method for synchronous generator core quality evaluation," IEEE Trans. Energy Convers., VOL. 19, NO. 3, , Sep. 2004, pp. 576–582

[7] M B Aimoniotis and A J Moses, "Evaluation of induced eddy currents in transformer sheets due to edge-burrs, employing computer aided design programs," in Athens Power Tech '93 Proc., 1993, VOL. 2, pp. 847–849

[8] R Mazurek, P Marketos, A J Moses and J N Vincent "Effect of artificial burrs on the total power loss of a three-phase transformer core", IEEE Trans. Magn., VOL. 46, NO. 2, 2010, pp.638 -641

[9] A J Moses and M Aimoniotis, "Effects of artificial edge burrs on the properties of a model transformer core," Physica Scripta, VOL. 39, 1989, pp. 391–393

[10] H Hamzehbahmani, A J Moses and F J Anayi "Opportunities and Precautions in Measurement of Power Loss in Electrical Steel Laminations Using the Initial Rate of Rise of Temperature Method" IEEE Trans. Mag. VOL. 49, NO. 3, March 2013, pp 1264- 1273

[11] E D Taylor, "The Measurement of Inter-laminar Resistance of Varnish-Insulated Silicon-Steel Sheet for Large Electrical Machines" Proceedings of the IEE - Part II: Power Engineering, VOL. 98, Issue 63, June 1951, pp. 377-385.

[12] J. G. Benford, "Separation of losses in oriented silicon steels from 0.13 to 0.34 mm thick," IEEE Trans. Magn. , vol. MAG-20, no. 3, pp.1545–1547, May 1984.

[13] A Bermúdez, D Gómez and P Salgado, "Eddy-Current Losses in Laminated Cores and the Computation of an Equivalent Conductivity", IEEE Trans Mahn , VOL. 44, NO. 12, Dec 2008, pp. 4730-4738

[14] R Lebourgeoisa, S Berenguerb, C Ramiarinjaonab and T Waeckerle "Analysis of the initial complex permeability versus frequency of soft nanocrystalline ribbons and derived composites", Journal of Magnetism and Magnetic Materials 254–255, 2003, pp. 191–194

[15] D P Arnold, I Z and M G Allen "Analysis and optimization of vertically oriented, through-wafer, laminated magnetic cores in silicon" Journal of Micromech. Microeng. NO 15, 2005, pp 971–977

[16] R Huang and D Zhang, "Experimentally Verified Mn–Zn Ferrites' Intrinsic Complex Permittivity and Permeability Tracing Technique Using Two Ferrite Capacitors", IEEE Trans Magn, VOL. 43, NO. 3, Mar 2007, pp 974-981

[17] K G Nilanga, B Abeywickrama, T Daszczynski, Y V Serdyuk and S M Gubanski," Determination of Complex Permeability of Silicon Steel for Use in High-Frequency Modeling of Power Transformers" IEEE Trans Magn, VOL. 44, NO. 4, April 2008, pp. 438-444

[18] A Geri, A Salvini and G M Veca "Displacement Eddy Current Computation in Magnetic Laminates" IEEE Trans Mag VOL. 30, NO. 2, March 1994, pp. 1075-1077

[19] G Loisos, A J Moses and P Beckley "Electrical Stress On Electrical Steel Coatings "JMMM 254–255 (2003) pp. 340–342

[20] J Wang, H Lin, Y Huang and L Huang, "Numerical Analysis of 3D Eddy Current Fields in Laminated Media Under Various Frequencies" IEEE Trans. Mag. VOL. 48, NO. 2, February 2012, pp 267-270

[21] C A Schulz, S p Duchesne, D Roger and J N Vincent, "Capacitive Short Circuit Detection In Transformer Core Laminations", Journal of Magnetism and Magnetic Materials 320 (2008) e911–e914

[22] A 937/A937 M-01, "Standard method for determining inter-laminar resistance of insulating coatings between two adjacent test surfaces"

[23] BS EN 10282:2001 "Method of test for the determination of surface insulation resistance of electrical sheet and strip"

[24] M Marion-Pera, A Kedous-Lebouc, T Waeckerle, and B Comut, "Characterization of SiFe Sheet Insulation" IEEE Trans Magn VOL 31. NO 4. July 1995, pp 2408-2415

[25] T L Mthombeni and P Pillay, "Physical basis for the variation of lamination core loss coefficients as a function of frequency and flux density" in Proc. IECON, Paris, France, Nov. 6–10, 2006, pp. 1381–1387

[26] G Bertotti, "General properties of power losses in soft ferromagnetic materials" IEEE Trans. Magn. VOL. 24, January1988 pp. 621-630

[27] M Ibrahim and P Pillay, "Advanced testing and modeling of magnetic materials including a new method of core loss separation for electrical machines " IEEE Trans on Industry Applications, VOL. 48, NO. 5, Sep/Oct 2012, pp. 1507 - 1515

[28] Y Chen and P Pillay, "An improved formula for lamination core loss calculations in machines operating with high frequency and high flu density excitation," IEEE 37th IAS Annual Meeting, VOL. 2, 13-18 Oct 2002, pp. 759–766

[29] D M Ionel, M Popescu, S J Dellinger, T J E Miller, R J Heideman, and M I McGilp, "On the Variation with Flux and Frequency of Core Loss Coefficients in Electrical Machine", IEEE Trans. Magn VOL. 42, NO. 3, May/June 2006 , pp. 658-666

[30] P J Tavner, R J Jackson "Coupling of discharge currents between conductors of electrical machines owing to laminated steel core", IEE Proceedings-B Electric Power Applications 135(6) Nov 1988, pp. 295-307